The Potential Role of Osteopontin in the Pathogenesis of Graves' Ophthalmopathy

Heng Lou,[1] Lian-Qun Wu,[1] Hao Wang,[2] Rui-Li Wei,[2] and Jin-Wei Cheng[1,2]

[1]Department of Ophthalmology, Eye and ENT Hospital, Fudan University, Shanghai, China
[2]Department of Ophthalmology, Shanghai Changzheng Hospital, Shanghai, China

Correspondence: Jin-Wei Cheng, Department of Ophthalmology, Eye and ENT Hospital, Fudan University, Shanghai, China; jinwei_cheng@yeah.net.

Received: January 6, 2021
Accepted: July 2, 2021
Published: September 21, 2021

Citation: Lou H, Wu LQ, Wang H, Wei RL, Cheng JW. The potential role of osteopontin in the pathogenesis of Graves' ophthalmopathy. *Invest Ophthalmol Vis Sci.* 2021;62(12):18. https://doi.org/10.1167/iovs.62.12.18

Purpose. The aim of this study is to evaluate the expression of osteopontin (OPN) and its relationship with relative cytokines in patients with Graves' ophthalmopathy (GO), and to observe the effect of OPN on orbital fibroblasts (OFs) proliferation, migration, and the expression of relative cytokines, as well as the signaling pathways involved in its effect.

Methods. The orbital adipose connective tissue was obtained from 24 patients with GO (12 cases of active GO, and 12 cases of inactive GO) and 12 healthy controls. OFs were isolated from orbital tissues obtained from patients with active GO who were undergoing orbital decompression surgery. Quantitative PCR and Western blot were performed to detect RNA and protein expression. The proliferation and cell migration rates of OFs were measured by methylthiazol tetrazolium (MTT) and the cell scratch test. Signaling pathway inhibitors, such as OPN monoclonal antibody 1A12, ERK1/2 inhibitor PD98059, and PI3K inhibitor LY294002, were applied to determine the involved pathways.

Results. The mRNA and protein levels of OPN were increased in orbital adipose connective tissue from patients with active GO than those from patients with inactive GO (2.83-fold increase, $P < 0.001$; 1.91-fold increase, $P < 0.05$). The OPN mRNA level was positively correlated with CD40 ligand (CD40L) and hyaluronan synthases 2 (HAS2) mRNA in patients with GO. OPN promoted proliferation and migration rate of OFs and induced vascular endothelial growth factor (VEGF) and collagen I mRNA expression, and the effects were inhibited by 1A12 or LY294002.

Conclusions. OPN in orbital adipose connective tissues were significantly increase in active GO, and there were significant correlations of OPN with CD40L and HAS2 mRNA levels in patients with GO. OPN promoted proliferation and migration of OFs and induced VEGF and collagen I mRNA expression in OFs through PI3K/Akt signaling pathway. This suggested a role for OPN in the pathogenesis of GO through the activation of OFs.

Keywords: osteopontin (OPN), orbital adipose connective tissue, Graves' ophthalmopathy (GO), orbital fibroblast (OF), vascular endothelial growth factor (VEGF), collagen I

Graves' ophthalmopathy (GO) is an autoimmune inflammatory disorder whose pathogenesis is very complicated and needs to be further explored. The natural clinical process follows a biphasic course with an active phase followed by a stable period. The orbital inflammatory response was intense in the active period, leading to collagen and glycosaminoglycan accumulation. Then, the orbital tissue expansion and extraocular muscle thickening as well as fibrosis were the results.[1] Current evidence suggests that orbital fibroblasts (OFs) play a vital role in orbital inflammation and tissue remodeling in GO. Enhanced proliferative activity, generation of inflammation mediators and excessive extracellular matrix (ECM), and differentiation into fat cells and myofibroblasts occur in OFs once activated by direct interaction with immune cells or by soluble cytokines.[2,3] Non-sulfated glycosaminoglycans (especially hyaluronic acid) and collagen content are increased in GO orbital tissue leading to tissue expansion and fibrosis. Hyaluronan synthases 2 (HAS2) is the main regulator of the hyaluronic acid synthesis in OFs from patients with GO.[4,5] The main objective of current clinical management is to reduce inflammation response in order to promote the transition from active to stable phase.

As a multifunctional cytokine, osteopontin (OPN) plays a part in normal physiology and participates in pathological process. It is expressed in fibroblasts,[6] osteoblasts, and T cells,[7] and has been proved to be a proinflammatory cytokine,[8] which is closely related with tissue fibrosis.[9] OPN also plays a pathogenetic role in many autoimmune diseases[10,11] (i.e. Grave's disease[12] and multiple sclerosis [MS]).[13,14] In the in vitro experiment, it has shown that OPN activated hepatic stellate cells and initiated the increase of collagen I leading to liver fibrosis, via activation of the PI3K/pAkt/NF-κB signaling pathway.[15] Recent studies had found that the level of serum OPN in patients with GD was significantly increased, as well as the OPN receptors (i.e. αv, $\beta 1$, $\beta 3$, and CD44), and many proinflammatory factors, such as CCL2, CCL3, CCL20, IL-1β, and IL-8.[12,16]

CD40/CD40 ligand (CD40L, also known as CD154, can act as a soluble cytokine) represents as an

important activation pathway initially implicated in T cell/B cell interactions.[17] Recently, it was reported that CD40 was overexpressed in OFs from patients with GO, and the CD40/CD40L co-stimulating pathway induced the activation of OFs.[18] The expression of plasma CD40L was increased in patients with GD and positively correlated with plasma OPN protein.[19]

An independently developed monoclonal antibody against OPN is 1A12 (patent application No. 200710039873.3). In the in vitro experiments, it was confirmed that 1A12 blocked the OPN-induced high expression of vascular endothelial growth factor (VEGF).[20] Animal experiments had also shown that 1A12 effectively inhibited the formation of new blood vessels and the growth and metastasis of tumors.[20,21] Therefore, 1A12 can alter OPN function and potentially has therapeutic value.

We hypothesize that OPN also plays a role in the pathogenesis of GO through the activation of OFs. This study aims to detect OPN in orbital adipose tissue in GO and to correlate OPN with GO disease activity, and to determine the effect of OPN on orbital fibroblasts through in vitro study.

Materials and Methods

Materials

The reagents used were as follows: OPN, OPN monoclonal antibody 1A12 (Institute of Oncology, Second Military Medical University, China); anti-vimentin, anti-CD45, anti-cytokeratin, and anti-factor VIII antibodies (Santa Cruz Biotechnology, Inc., Dallas, TX, USA); ERK1/2 inhibitor PD980592, and PI3K inhibitor LY294002 (Sigma-Aldrich, St. Louis, MO, USA).

Subjects

Orbital adipose connective tissue explants were collected from 36 participants, which were recruited consecutively from the Department of Ophthalmology, Shanghai Changzheng Hospital, after informed consent was approved by the institutional review board.

Twenty-four patients were diagnosed with GO, based on Bartley diagnosis criteria.[22] Twelve of them were diagnosed with active GO who accepted the emergency orbital decompression to save the sight of the patients due to dysthyroid optic neuropathy or exposure keratitis. The rest of them were patients with inactive GO. The activity of GO was evaluated by the clinical activity score (CAS), with active GO being defined as CAS≥3/7 and inactive GO defined as CAS≤2/7.[23] Twelve individuals undergoing plastic surgery were included as normal controls. The clinical characteristics of these patients are shown in Table 1. Three different OF culture strains were obtained from three patients diagnosed with active GO (see Table 1, No. 1–3).

The following conditions were excluded: patients with other systemic autoimmune or inflammatory diseases and patients with diabetes mellitus.

All 12 patients with active GO were initially diagnosed and treated for hyperthyroidism, 6 of them were women, median age 49 years (range = 32–64 years). Five of the patients were current smokers, one quit smoking 12 months ago, the other 6 had never smoked. Time from onset of Graves' disease to decompression surgery ranged from 10 to 72 months. Three patients had received radioiodine treatment, one had received thyroid surgery 6 months ago. Nine patients were taking antithyroid drugs at the time of the surgery, and the other patients stopped taking antithyroid drugs 8 to 36 months ago. One of the 12 patients had never received glucocorticoids, the remaining 11 patients had been treated with glucocorticoids in the past but had discontinued use several months before the surgery. Two patients had received orbital radiation 2 months before decompression surgery.

All 12 patients with inactive GO were initially diagnosed and treated for hyperthyroidism, 7 of them were women, median age 43 years (range = 20–60 years). One of the patients quit smoking 24 months ago, and the rest of them had never smoked. Time from onset of Graves' disease to decompression surgery ranged from 12 to 132 months. One patient had received radioiodine treatment. All of them were taking antithyroid drugs at the time of the surgery. Three of them had been treated with glucocorticoids in the past but had discontinued use 6 to 12 months before the surgery, the other 9 patients had never received glucocorticoids. One patient had received orbital radiation 36 months before decompression surgery.

All the subjects included were euthyroid and had normal TSH levels within 6 months at the time of orbital fat harvesting. There was no significant difference in gender ratio or age between the groups. These activities were undertaken after informed consent was obtained from the participants, and the research protocol adhered to the tenets of the Declaration of Helsinki.

RNA Isolation and Quantitative RT-PCR

Orbital adipose connective tissue explants were washed by normal saline immediately upon harvesting, and then frozen in liquid nitrogen within 5 minutes until use. Total RNA was extracted from orbital specimen and OFs using TRIpure Reagent (Aidlab Biotechnologies Co., Ltd., Beijing, China) and was solubilized by RNase free water. RNA was converted into first-strand cDNA with the reverse transcription kit (Takara, Shiga, Japan). Real time (RT)-PCR was performed using 2 × Real Time PCR Mix (Probe; Aidlab Biotechnologies Co., Ltd.) on an Applied Biosystems 7500HT Real-Time PCR system according to the manufacturer's protocol. PCR array data were calculated by the ΔΔCt method. The endogenous reference gene GAPDH was used as the negative control for normalization treatment, and there was no difference in GAPDH gene expression levels among the three groups.

All PCR primers and probes (TaqMan Gene Expression Assay) for OPN, CD40L, CD44, NF-κB, CCL20, collagen I, HAS2, and VEGF were designed by Sangon Biotech (Sangon, Shanghai, China; Table 2).

Western Blot Analysis of OPN Protein

Orbital samples were washed in pre-cold saline and the vascular tissue was cut off as much as possible, then solubilized by RIPA Lysis Buffer (Aidlab Biotechnologies Co., Ltd.) and every 10 mL was supplemented with a protease inhibitor, then protein concentrations in the extracts were measured with BCA Protein Assay Kit (Aidlab Biotechnologies Co Ltd.). Equal volumes of extracts were separated by SDS-PAGE, and then transferred onto the polyvinylidene fluoride (PVDF) membranes. The membranes were sealed using 5% non-fat milk solution for 2 hours at 24°C. The blots were then incubated with primary antibodies for 24 hours at 4°C and then incubated with secondary antibodies for 2

Investigative Ophthalmology & Visual Science

Table 1. Clinical Characteristic of the Patients

Patients	Age	Sex	Smoking History	Onset of GD (Months)	Radioiodine Rxa (Months)	Thyroid Surgery	Antithyroid Drug Rxa	Onset of Clinical GO (Months)	Prednisone Rx	Duration of Prednisone Treatment	Orbital Radiation Rxa	Surgical Procedure	Clinical Activity Score	TRAB (IU/L)
Active GO														
1	48	M	Never	24	Never	Never	Current (24 months duration)	24	Stopped 2 months prior (500 mg/w × 6, 250 mg/w × 18)	6 months	Never	Emergency orbital decompression	7	9.2
2	44	M	Current (15/d, 18 years)	24	Never	Never	Current (24 months duration)	24	Stopped 6 months prior (500 mg/w × 8, 250 mg/w × 4)	3 months	Never	Emergency orbital decompression	3	40.0
3	55	F	Never	36	36	Never	36 months ago	36	Never	Never	Never	Emergency orbital decompression	7	0.9
4	52	F	Never	10	8	6 months ago	8 months ago	3	Stopped 2 months prior (Prednisone p.o.)	10 days	Never	Emergency orbital decompression	6	7.7
5	57	F	Current	72	Never	Never	Current (12 months duration)	12	Stopped 1 months prior (1500 mg/w × 4, 250mg/w × 4)	Not clear	Stopped 2 months prior	Emergency orbital decompression	3	4.7
6	64	M	Current (20/d, 30 years)	24	Never	Never	Current (24 months duration)	24	Stopped 12 months prior (not clear)	Not clear	Never	Emergency orbital decompression	6	24.1
7	36	F	Never	36	Never	Never	Current (24 months duration)	36	Stopped 2 months prior (500 mg/w × 6, 250 mg/w × 6)	3 months	Never	Emergency orbital decompression	5	34.3
8	47	M	Current	12	Never	Never	Current (12 months duration)	24	Stopped 6 months prior (500 mg/w × 8, 250 mg/w × 4)	3 months	Never	Emergency orbital decompression	6	7.05
9	51	F	Never	24	Never	Never	24 months ago	18	Stopped 2 months prior (Prednisone p.o.)	1 month	Never	Emergency orbital decompression	7	0.6
10	32	F	Never	18	12	Never	Current (36 months duration)	12	Stopped 6 months prior (500 mg/w × 8, 250 mg/w × 8)	4 months	Stopped 2 months	Emergency orbital decompression	6	0.7
11	56	M	Stopped 12 months prior	34	Never	Never	Current (12 months duration)	12	Stopped 12 months prior (not clear)	Not clear	Never	Emergency orbital decompression	5	3.6
12	53	M	Current	28	Never	Never	Current (24 months duration)	24	Stopped 1 month prior (2500 mg/w × 6)	1.5 months	Never	Emergency orbital decompression	6	2.0
Inactive GO														
1	36	F	Never	132	108 months ago	Never	Current (132 months duration)	132	Never	Never	Never	Orbital decompression	0	3.6
2	20	F	Never	21	Never	Never	Current (21 months duration)	14	Never	Never	Never	Orbital decompression	0	5.3
3	63	M	Never	120	Never	Never	Current (120 months duration)	48	Never	Never	Never	Orbital decompression	0	10.6
4	23	M	Never	96	Never	Never	Current (96 months duration)	96	Never	Never	Never	Orbital decompression	0	1.2
5	34	F	Never	24	Never	Never	Current (24 months duration)	36	Stopped 6 months prior	2 months	Never	Orbital decompression	0	3.3

Table 1. Continued

Patients	Age	Sex	Smoking History	Onset of GD (Months)	Radioiodine Rxa (Months)	Thyroid Surgery	Antithyroid Drug Rxa	Onset of Clinical GO (Months)	Prednisone Rx	Duration of Prednisone Treatment	Orbital Radiation Rxa	Surgical Procedure	Clinical Activity Score	TRAB (IU/L)
6	48	M	Never	12	Never	Never	Current (12 months duration)	12	Stopped 8 months prior	5 months	Never	Orbital decompression	0	0.5
7	54	F	Never	70	Never	Never	Current (70 months duration)	48	Never	Never	Stopped 36 months prior	Orbital decompression	0	15.1
8	46	F	Never	40	Never	Never	Current (40 months duration)	36	Never	Never	Never	Orbital decompression	0	11.8
9	45	M	Stopped 24 months prior	24	Never	Never	Current (24 months duration)	24	Stopped 12 months prior	3 months	Never	Orbital decompression	0	15.9
10	50	M	Never	36	Never	Never	Current (36 months duration)	36	Never	Never	Never	Orbital decompression	0	0.7
11	36	F	Never	48	Never	Never	Current (48 months duration)	24	Never	Never	Never	Orbital decompression	0	14.5
12	60	F	Never	52	Never	Never	Current (52 months duration)	52	Never	Never	Never	Orbital decompression	0	10.8
Controls														
1	63	M	Never	Never	Never	Never	Never	Never	Never	Never	Never	Orbital adipose prolapse repair		
2	52	F	Never	Never	Never	Never	Never	Never	Never	Never	Never	Trichiasis repair		
3	61	F	Never	Never	Never	Never	Never	Never	Never	Never	Never	Trichiasis repair		
4	48	F	Never	Never	Never	Never	Never	Never	Never	Never	Never	Ptosis repair		
5	52	F	Never	Never	Never	Never	Never	Never	Never	Never	Never	Trichiasis repair		
6	61	F	Never	Never	Never	Never	Never	Never	Never	Never	Never	Trichiasis repair		
7	38	M	Never	Never	Never	Never	Never	Never	Never	Never	Never	Trichiasis repair		
8	51	F	Never	Never	Never	Never	Never	Never	Never	Never	Never	Trichiasis repair		
9	30	M	Never	Never	Never	Never	Never	Never	Never	Never	Never	Ptosis repair		
10	54	F	Never	Never	Never	Never	Never	Never	Never	Never	Never	Trichiasis repair		
11	57	F	Never	Never	Never	Never	Never	Never	Never	Never	Never	Trichiasis repair		
12	60	M	Never	Never	Never	Never	Never	Never	Never	Never	Never	Trichiasis repair		

Table 2. All Primers and Probes Sequences

Geans	Primer_F (5′-3′)	Primer_R (5′-3′)	Primer Probe (5′-3′)
OPN	TGAAACGAGTCAGCTGGATG	TGAAATTCATGGCTGTGGAA	AGAGCAATGAGCATTCCGATGTGATTG
CD40L	AATTGCGGCACATGTCATAA	CTTCCCGATTGGAACAGAAG	TAACCCTGGAAAATGGGAAACAGCTGA
CD44	AAGGTGGAGCAAACACAACC	AGCTTTTTCTTCTGCCCACA	CAGTTTGCATTGCAGTCAACAGTCGAA
NF-κB	CCTGGATGACTCTTGGGAAA	TCAGCCAGCTGTTTCATGTC	TAGATATGGCCACCAGCTGGCAGGTAT
CCL20	GCGCAAATCCAAAACAGACT	CAAGTCCAGTGAGGCACAAA	TGGCTTTTCTGGAATGGAATTGGACAT
CollagenI	GTGCTAAAGGTGCCAATGGT	ACCAGGTTCACCGCTGTTAC	CTGGTATTGCTGGTGCTCCTGGCTT
HAS2	GCCTCATCTGTGGAGATGGT	ATGCACTGAACACACCCAAA	AGGTGTTGGGGGAGATGTCCAGATTTT
VEGF	GCAGAATCATCACGAAGTGGT	TGAAGATGTACTCGATCTCATCA	CCCTGGTGGACATCTTCCAGG
GAPDH	CAATGACCCCTTCATTGACC	TTGATTTTGGAGGGATCTCG	ATGTTCCAATATGATTCCACCCATGGC

hours at 4°C. Scans of the full films used to generate Western blot data were obtained by Amersham Imager 600 (GE Healthcare Bio-Sciences AB, Sweden). The protein expression levels were quantified by measuring band intensities using Image J software (National Institutes of Health [NIH], Bethesda, MD, USA). The values were normalized to β-actin.

Cell Culture

Surgical tissue explants were transported to the laboratory cell room for cell culture as soon as possible (within 6 hours) in DMEM (Hyclone Co., Logan UT, USA) under low temperature. Primary culture cells were adhered and proliferated in 10% FBS (Hyclone Co., USA). The cells need to be identified by immunostaining and flow cytometry with positive staining of vimentin and collagen, as well as negative staining of CD45, cytokeratin, or factor VIII tested by anti-vimentin, anti-CD45, anti-cytokeratin, and anti-factor VIII antibodies (Santa Cruz Biotechnology, Inc., Dallas, TX, USA). Cells then passaged by trypxin (Sigma Co., USA) and stable passages (passage 4 to 7) were used for following experiments.

The following cell experiments were divided into five groups, the control group (normal medium), OPN treatment group (5 µM), OPN + LY294002 (5 µM + 20 µM) treatment group, OPN + PD980592 (5 µM + 20 µM) treatment group, and OPN + 1A12 treatment group (5 µM + 20 µg/mL).

Cell Proliferation

Approximately, 1000 cells per well were seeded in 96-well plates in media containing 10% FBS and incubated for 0 hours, 24 hours, 48 hours, 72 hours, and 96 hours. On the indicated days, 3-(4,5)-dimethylthiahiazo(-z-y1)-3,5- diphenytetrazoliumromide (MTT) reagent (Sangon, China) was added to each well, and cells were incubated for 4 hours at 37°C. Supernatants were then removed and 100 µL of DMSO (Sangon, China) was added per well to dissolve formazan crystals. Optical densities (ODs) were measured at 490 nm using an automatic microplate reader (Gene Co., Ltd., Hong Kong). The OD is proportional to the number of OFs. Relative cell proliferation rates were calculated by the following formula: cell proliferation rate (%) = OD day N / OD day 0 × 100%.

Cell Scratching

Cultures of OFs cells were seeded at a density of 1×10^6 cells/well in 12-well plates and incubated until confluence. Thereafter, the incubated cell cultures were scratched with a p200 pipette tip in the middle of the wells and the suspension cells were washed off with PBS. The scratch area was analyzed by microscope and images were captured at times 0 hours, 12 hours, and 24 hours. The scratch areas were quantified using Image J software.

Statistical Analysis

SPSS 22.0 was used to analyze the experimental data, Shapiro-Wilk Test was used to determine whether the data follow normal distribution. The Levene test was used to analyze the homogeneity of variance. Kruskal-Wallis H with the Bonferroni's post hoc test was used to analyze data with non-normal distribution or nonheterogeneity variance from three groups. Multiple logistic regression analysis was used to test whether smoking has a significant effect on OPN, CD40L, collagen I, and HAS2 mRNA expression. Spearman correlation analysis was used in the study of correlations among OPN mRNA and the other cytokines. One-way ANOVA followed by Tukey's post hoc test was used to compare multiple groups with normal distribution and heterogeneity variance.

Results

The mRNA Levels of OPN in Orbital Adipose Connective Tissue

There was a statistical difference among the three groups ($H = 20.02$, $P < 0.001$). The mRNA level of OPN in orbital adipose connective tissues from patients with active GO was significantly higher than those from patients with inactive GO (2.83-fold increase, $P < 0.001$, $n = 12{:}12$), as well as from healthy subjects (1.94-fold increase, $P < 0.05$, $n = 12{:}12$). There was no significant difference of the mRNA levels of OPN in orbital adipose connective tissues between from patients with inactive GO and from healthy subjects (0.69-fold increase, $P > 0.05$, $n = 12{:}12$; Fig. 1).

The Protein Levels of OPN in Orbital Adipose Connective Tissue

The previous experiment demonstrated the increased mRNA level of OPN in orbital tissue from patients with active GO when compared with those from patients with inactive GO and healthy controls. In the next step, we tested the protein level of OPN in orbital tissue by Western blot (Fig. 2).

There was a statistical difference of OPN protein levels among the three groups ($H = 9.641$, $P < 0.01$). OPN protein expression in orbital adipose connective tissue from patients with active GO was significantly higher than those from patients with inactive GO (1.91-fold increase, $P < 0.05$, $n = 12{:}12$).

Investigative Ophthalmology & Visual Science

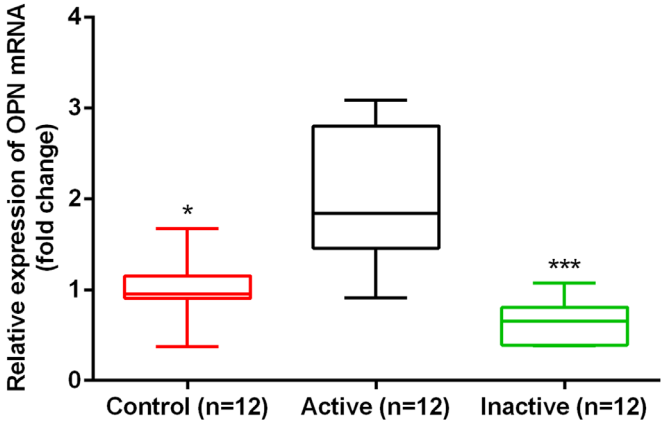

Figure 1. The relative expression (fold change) of OPN RNA in orbital adipose connective tissue from patients with active GO, patients with inactive GO and healthy subjects. The RT-PCR assay was performed three times for each sample. All the results were shown as mean ± SD. Statistical analysis has been performed by Kruskal-Wallis H with the Bonferroni's post hoc test (n = 12:12:12). *P < 0.05, ***P < 0.001: statistically significant difference compared with the active GO group.

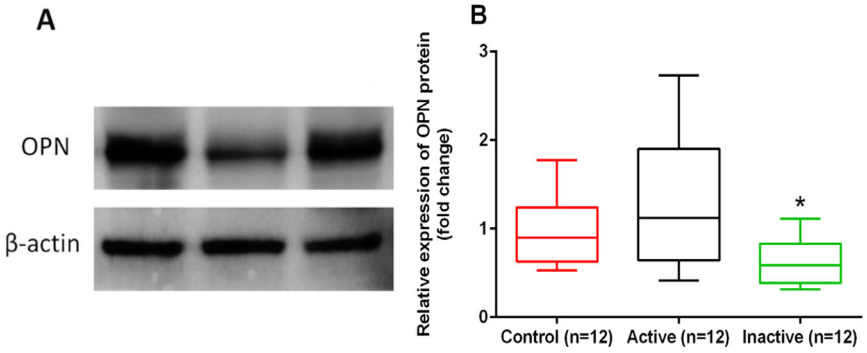

Figure 2. Western blot (**A**) and densitometric analysis (**B**) (fold change) of the expression of OPN protein in orbital adipose connective tissue from patients with active GO, patients with inactive GO and healthy subjects. The Western blot assay was performed three times for each sample. All the results were shown as mean ± SD. Statistical analysis has been performed by Kruskal-Wallis H with the Bonferroni's post hoc test (n = 12:12:12). *P < 0.05: statistically significant difference compared with the patients with active GO group.

There was no significant difference of OPN protein expression in orbital adipose connective tissue from patients with active GO (1.25-fold increase, $P > 0.05$, n = 12:12) and patients with inactive GO (0.65-fold increase, $P > 0.05$, n = 12:12), when compared with those from healthy subjects.

The mRNA Levels of Inflammatory Cytokines and Correlation with OPN Level

Then, the mRNA levels of several inflammatory cytokines, such as CD40L, collagen I, HAS2, NF-κB, CCL20, and CD44 were detected, and the correlation coefficients between logarithmically transformed OPN levels and the inflammatory cytokines of GO were calculated. There were statistical differences among the three groups of CD40L, collagen I, and CD44 mRNA levels (H = 20.02, $P < 0.001$; H = 12.907, $P < 0.01$; H = 20.122, $P < 0.001$; Fig. 3).

The mRNA levels of CD40L and collagen I in orbital tissue from patients with active GO were significantly higher than those from patients with inactive GO (3.14-fold increase, $P < 0.01$, n = 12:12; 2.75-fold increase, $P < 0.01$, n = 12:12) and healthy subjects (5.03-fold increase, $P < 0.01$, n = 12:12; 1.87-fold increase, $P < 0.05$, n = 12:12). There was no significant difference of the mRNA levels of CD40L and collagen I between patients with inactive GO and healthy subjects (1.60-fold increase, $P > 0.05$, n = 12:12; 0.68-fold increase, $P > 0.05$, n = 12:12).

The mRNA levels of CD44 in orbital adipose connective tissues from healthy subjects were higher than those from patients with active (1.51-fold increase, $P < 0.05$, n = 12:12) and inactive (2.48-fold increase, $P < 0.001$, n = 12:12) GO, and there was no significant difference between patients with active GO and patients with inactive GO ($P > 0.05$).

There was no significant difference of the mRNA level of HAS2, NF-κB, and CCL20 in orbital adipose connective tissues among the three groups ($P > 0.05$).

The Spearman correlation analysis revealed that the expression of OPN mRNA positively correlated with CD40L (r = 0.80, $P < 0.001$), collagen I (r = 0.61, $P < 0.01$), and HAS2 mRNA (r = 0.73, $P < 0.001$) in orbital adipose connective tissue from patients with active and inactive GO (n = 24; Fig. 4).

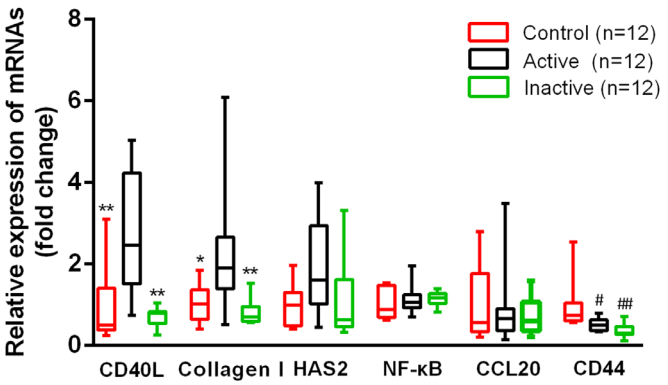

Figure 3. The relative expression (fold change) of CD40L, collagen I, HAS2, NF-κB, CCL20, and CD44 RNA in orbital adipose connective tissue from patients with active GO, patients with inactive GO and healthy subjects. The RT-PCR assay was performed three times for each sample. All the results were shown as mean ± SD. Statistical analysis has been performed by Kruskal-Wallis H with the Bonferroni's post hoc test (n = 12:12:12). *P < 0.05, **P <0.01, ***P < 0.001: statistically significant difference compared with the patients with active GO group. $^{\#}P$ < 0.05, $^{\#\#}P$ <0.001: statistically significant difference compared with the control group.

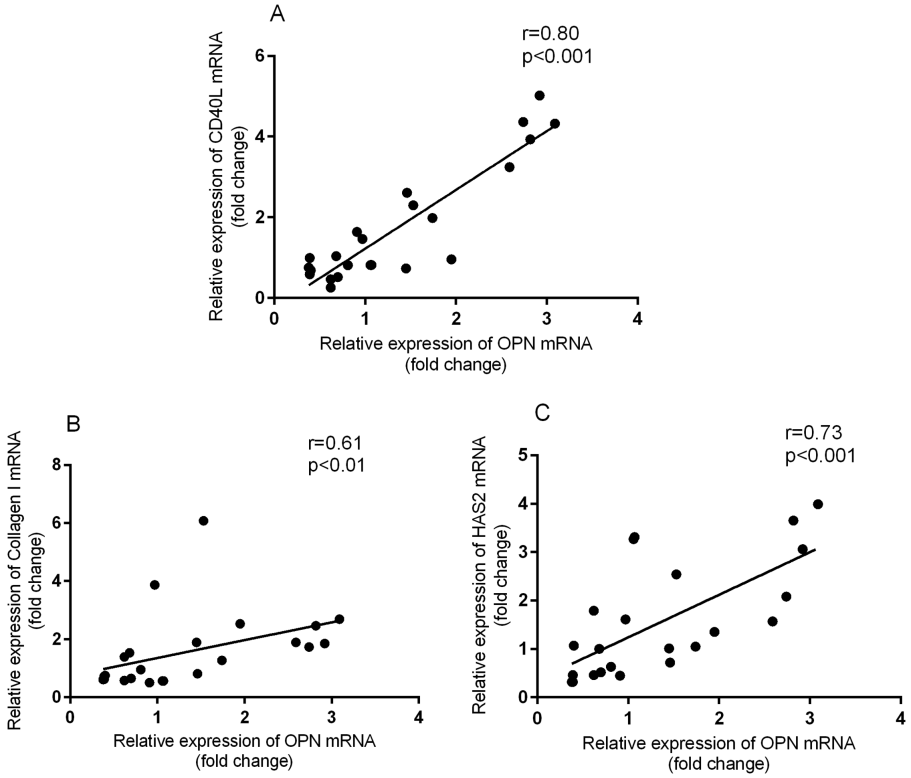

Figure 4. Spearman correlation analysis of the mRNA levels between OPN and CD40L (r = 0.80, P < 0.001) (**A**), OPN and collagen I (r = 0.61, P < 0.01) (**B**), OPN and HAS2 mRNA (r = 0.73, P < 0.001) (**C**), in orbital adipose connective tissue from all patients with active and inactive GO (n = 24).

The Relationship Among Smoking Status, TRAB Levels CAS Score, and Cytokine Levels

Smokers have a greater chance of developing GO and more severe forms of the ophthalmopathy. Six out of the 12 patients with active GO were current or former smokers, and 1 out of the 12 patients with inactive GO smoked before (see Table 1). Multiple logistic regression analysis showed that smoking had no significant effect on OPN (β = -0.205, 95% confidence interval [CI] = -1.159 to 0.369, P =0.293), CD40L (β = -0.102, 95% CI = -1.407 to 0.774, P =0.551), collagen I (β = 0.325, 95% CI = -0.470 to 2.282, P =0.184), and HAS2 (β = -0.287, 95% CI = -2.076 to 0.639, P =0.281) mRNA expression levels in patients with GO.

There was no significant difference of the TSHR antibody (TRAB) levels between patients with active and inactive GO (P > 0.05; see Table 1). Because all patients with inactive GO had a CAS score of 0, the Spearman correlation analysis was only performed on patients with active GO. There was no linear correlation of TRAB levels, and CAS score with OPN

Investigative Ophthalmology & Visual Science

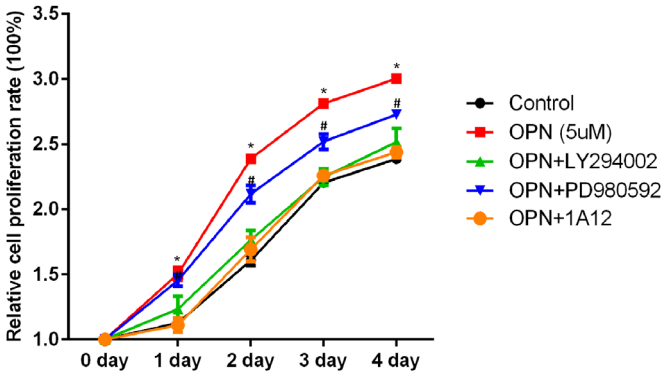

Figure 5. OFs proliferation rate curve of control, OPN, OPN + LY294002, OPN + PD980592, and OPN + 1A12 cultures at time of day 0, day 1, day 2, day 3, and day 4. All the results were shown as mean ± SD ($n = 3$), which were three separate experiments performed in triplicate. $^{*}P < 0.001$: statistically significant difference compared with the other four groups. $^{\#}P < 0.001$: statistically significant difference compared with the other three groups except the OPN treatment group.

(r = −0.064, $P = 0.768$; r = 0.165, $P = 0.608$) and other inflammatory cytokines mRNA ($P > 0.05$).

OPN Promotes Proliferation Rate of OFs

The results showed enhanced OFs proliferation rate starting from day 1 in the OPN group, and a dramatic reduction of OFs proliferation with the addition of LY294002 and 1A12 to the level of the control group ($P < 0.001$). The OFs proliferation rate of the OPN + PD980592 treatment group was higher than that of the other three groups ($P < 0.001$), except of the OPN treatment group. There was no significant difference among the OPN + 1A12, OPN + LY294002 treatment group, and the control group ($P > 0.05$, Fig. 5).

OPN Promotes Migration Rate of OFs

At 0 hours, 12 hours, and 24 hours after the scratch, cell migration photographs and relative migration distance in the low-power field were shown in Figure 6-1 and Figure 6-2, respectively. At the 12th and 24th hours, the OFs migration distance of OPN and the OPN + PD980592 treatment group was significantly higher than that of the other three groups ($P < 0.001$), whereas the difference between OPN + 1A12, OPN + LY294002, and the control group was not statistically significant ($P > 0.05$).

OPN Induces VEGF and Collagen I mRNA Expression of OFs

After 48 hours of the culture, the VEGF mRNA expression in the control group was onefold. When OPN was introduced to the cell culture, VEGF mRNA expression increased by 2.25-fold ($P < 0.001$), the increase of VEGF mRNA was completely eliminated by the addition of an PI3K inhibitor (LY294002) and monoclonal antibody toward OPN (1A12), but not by the addition of the ERK1/2 inhibitor (PD980592; Fig. 7).

After 48 hours of the culture, the collagen I mRNA expression in the control group was onefold, the expression was significantly increased when OPN was introduced to cell culture (2.66-fold increase, $P < 0.001$). The effect was completely eliminated by the addition of a PI3K inhibitor (LY294002) and monoclonal antibody toward OPN (1A12), but not by the addition of the ERK1/2 inhibitor (PD980592; Fig. 8).

Discussion

As an autoimmune inflammatory disorder, GO has a complicated management and its immunopathogenesis is poorly understood. Currently, the main treatments for active GO have been systemic corticosteroids and orbital radiation to control disease progression. However, due to lack of specificity and limitation of side effects, it is easy to relapse. Therefore, further studies on the pathogenesis of GO are needed to find newly effective treatments.

In early active GO, T cells infiltrate into the orbital tissue and activate OFs via the secretion of inflammatory mediators. T-helper 1 (Th1)-lymphocytes dominated in the active phase of GO, whereas in the stage of tissue remodeling and fibrosis at the later stage of disease, T-helper 2 (Th2)-lymphocytes and associated cytokines gradually became predominant.[24–27] OPN was reported to be a proinflammatory cytokine, which promoted Th1 response and inhibited Th2 response.[8,28,29] The binding of OPN and CD44 mediated chemotaxis and adhesion of fibroblasts, T cells, and bone marrow cells.[30–32] Serum OPN protein levels was elevated among patients with Grave's disease and correlated with fT3 and fT4 strongly.[16]

The proliferation of OFs, production of extracellular matrix, and differentiation into adipocytes and myofibroblasts are important factors for the expansion and fibrosis of the orbital tissues in GO.[33–35] CD40-CD40L binding is involved in physical interactions between OFs and T-lymphocytes in GO. In studies performed by our research group, it was found that intercellular adhesion molecular-1 (ICAM-1), vascular cell adhesion molecular-1 (VCAM-1), and E-selectin expression in cultured OFs from patients with GO were enhanced by CD40L stimulation.[36,37]

In the present study, we detected the overexpression of OPN, CD40L, and collagen I mRNA as well as OPN protein in orbital tissues from patients with active GO, and the levels of OPN mRNA from patients with GO have significant correlations with CD40L and collagen I mRNA. The gene expression of OPN was positively correlated with the expression of HAS2. However, there appeared to be no significant difference of HAS2 mRNA expression between active and inactive GO. As the main regulator of the hyaluronic acid synthesis

Investigative Ophthalmology & Visual Science

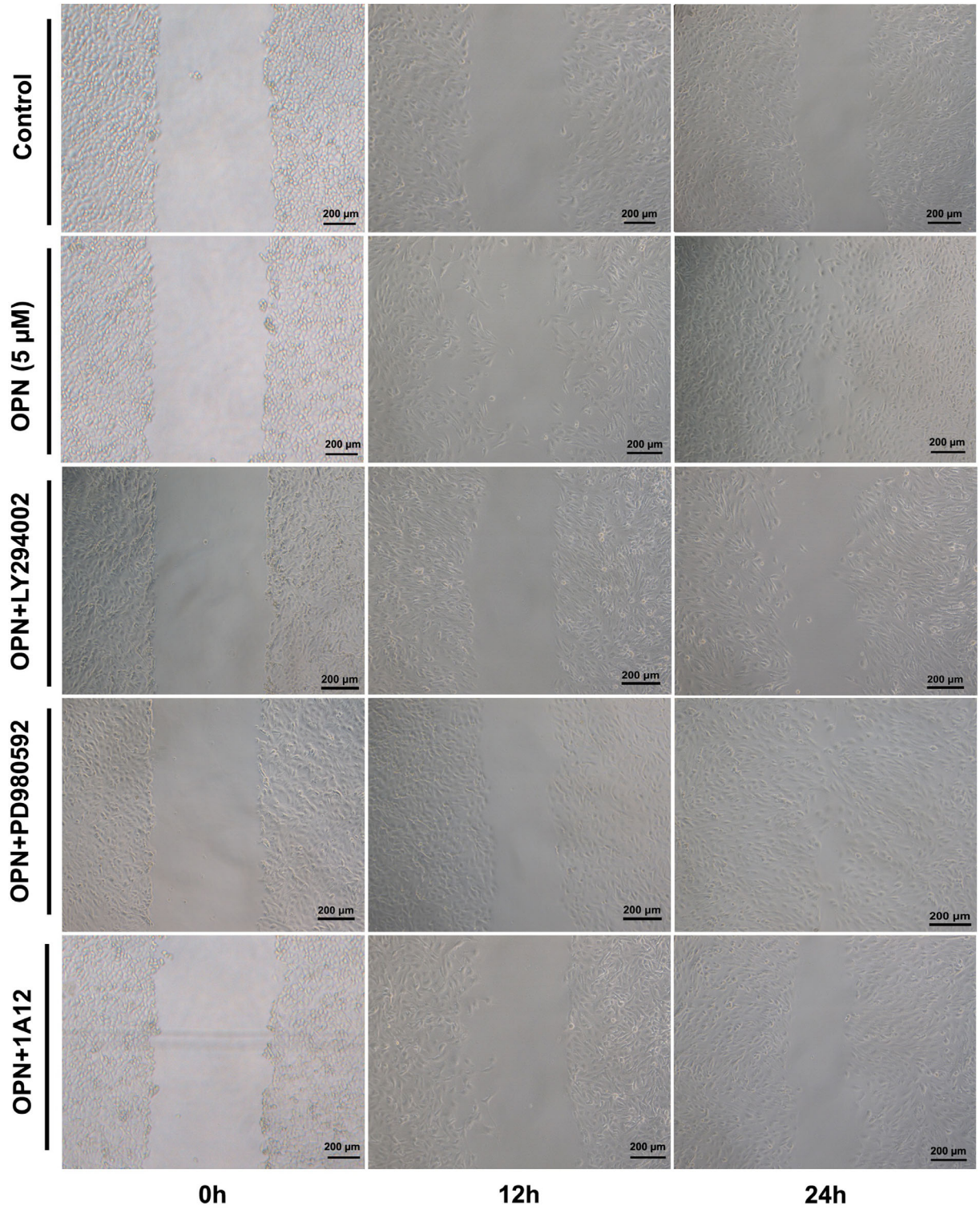

Figure 6-1. Representative images of scratch areas of OFs of control, OPN, OPN + LY294002, OPN + PD980592, and OPN + 1A12 cultures at time 0 hours, 12 hours, and 24 hours.

in OFs from patients with GO,[38,39] HAS2 may be expressed in both active and inactive GO. Otherwise, the limitations of the present study, such as small sample size, might be a potential reason for the negative result.

We also did not find any significant difference of CD44 and NF-κB mRNA expression between patients with active and inactive GO. Previous study had shown that OPN upregulated collagen I via $\alpha v\beta 3$ engagement in liver fibrosis.[15] OPN increased the expression of CCL20 in CD4+T cells from patients with GD via the $\beta 3$ integrin receptor.[40] Therefore, the binding receptor of OPN, which exerted its function in OFs from patients with GO need to be further explored. In

Investigative Ophthalmology & Visual Science

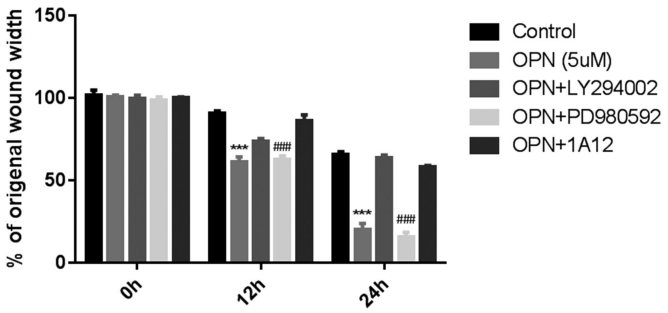

Figure 6-2. Percentage of scratch areas of OFs of control, OPN, OPN + LY294002, OPN + PD980592, and OPN + 1A12 cultures at time 0 hours, 12 hours, and 24 hours. All the results were shown as mean ± SD ($n = 3$), which were three separate experiments performed in triplicate. Statistical analysis has been performed by 1-way ANOVA followed by Tukey's post hoc test. $^{***}P < 0.001$: statistically significant difference compared with the other three groups except the OPN + PD980592 treatment group. $^{\#\#\#}P < 0.001$: statistically significant difference compared with the other three groups except the OPN treatment group.

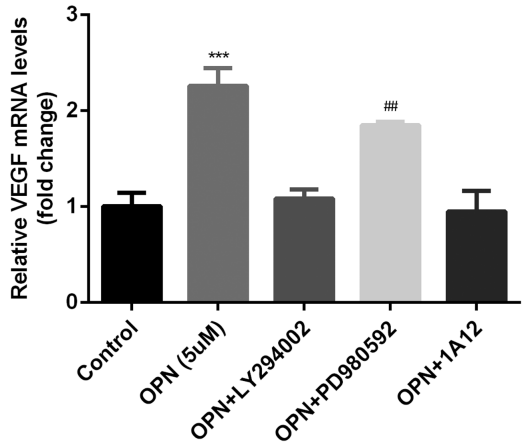

Figure 7. The relative expression (fold change) of VEGF mRNA in OFs of control, OPN, OPN + LY294002, OPN + PD980592, and OPN + 1A12 cultures after 48 hours. The cells were harvested after stimulation was completed, and RT-PCR analysis was performed with the total mRNA extracted from the OFs. Values are presented as the mean ± SD of three separate experiments. Statistical analysis has been performed by 1-way ANOVA followed by Tukey's post hoc test. $^{***}P < 0.001$: statistically significant difference compared with the other three groups except the OPN + PD980592 treatment group. $^{\#\#}P < 0.01$: statistically significant difference compared with the other three groups except the OPN treatment group.

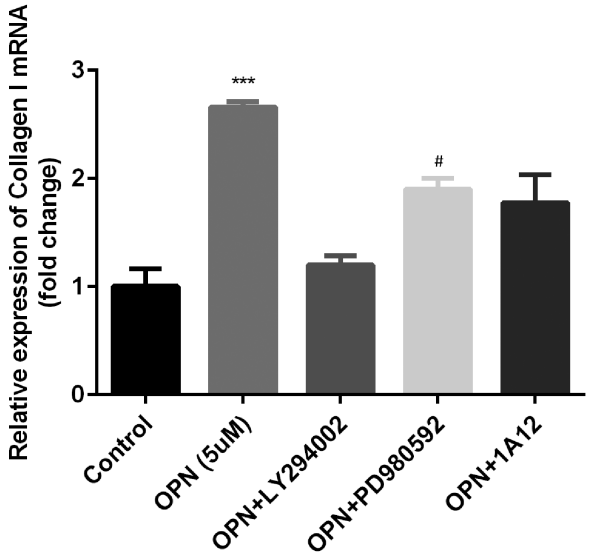

Figure 8. The relative expression (fold change) of collagen I mRNA in OFs of control, OPN, OPN + LY294002, OPN + PD980592, and OPN + 1A12 cultures after 48 hours. The cells were harvested after stimulation was completed, and RT-PCR analysis was performed with the total mRNA extracted from the OFs. Values are presented as the mean ± SD of three separate experiments. Statistical analysis has been performed by 1-way ANOVA followed by Tukey's post hoc test. $^{***}P < 0.001$: statistically significant difference compared with the other three groups except the OPN + PD980592 treatment group. $^{\#}P < 0.05$: statistically significant difference compared with the control and OPN + LY294002 treatment groups.

patients with GD, the expression of cytokine genes downstream of NF-κB was elevated in peripheral blood mononuclear cells (PBMCs), and OPN could activate NF-κB signaling in vitro.[12] Previous experiments had shown that cytokines played pathophysiological roles through NF-κB signaling in vitro.[41–43] However, in this present study, we found that the levels of NF-κB mRNA did not increase in orbital adipose connective tissues from patients with GO. We hypothesized that OPN might not play its effect through the NF-κB pathway in orbital adipose connective tissues of active GO, and an in vitro study confirmed that OPN activated OFs through PI3K/Akt signaling pathway.

VEGF, as a potent stimulator of glycosaminoglycan accumulation and edema formation,[45] has been reported to be increased in serum and orbital tissues among patients with active GO, which could reflect the degree of ocular inflammatory activity.[46,47] In vitro experiments had confirmed that OPN enhanced the expression of collagen I in hepatic stellate cells to expand liver fibrosis and promoted the expression of VEGF and induce angiogenesis through the PI3K/Akt signaling pathway.[15,48] In the present study, we found that OPN activated OFs and induced VEGF and collagen I mRNA expression in OFs through the PI3K/Akt signaling pathway.

Smoking, as a major risk factor for GO, is related to the occurrence and severity of GO. However, our study was too small to show an effect of smoking, and there was not a positive association of smoking status or cigarette pack years with OPN and other inflammatory cytokines' mRNA expression levels.

Investigative Ophthalmology & Visual Science

TRAB plays a unique role in the development of autoimmune hyper- and hypothyroidism.[44] In this study, we found that there was no significant difference of the TARB levels between patients with active and inactive GO, and there was no linear correlation between TRAB levels and OPN and other inflammatory cytokines mRNA. Larger sample size experiments are needed to verify the results.

There were various data in this study that supported OPN's role in the pathogenesis of GO, perhaps not the correlation between OPN mRNA/protein level and CAS, which might also be because of the small sample size.

There are several limitations to the current study that merit consideration. First of all, the sample size of each group was small. Second, the OFs were only obtained from three patients with active GO. Further studies with larger sample size may be needed in the future.

Conclusion

Our study has shown that the mRNA and protein levels of OPN in orbital adipose connective tissues, as well as CD40L and collagen I mRNA, increased significantly among patients with active GO. Furthermore, there were significant linear correlations of OPN with CD40L, collagen I, and HAS2 mRNA levels in patients with GO. Additionally, we also found that OPN promoted proliferation and migration of OFs and induced VEGF and collagen I mRNA expression in OFs through the PI3K/Akt signaling pathway. Overall, these findings indicated that OPN might play an important role in the pathogenesis of GO, especially in the active period through the activation of OFs, to promote orbital inflammation and the remodeling and fibrosis in orbital tissue, through the PI3K/Akt signaling pathway.

Acknowledgments

Supported by the National Natural Science Foundation of China (81170874).

Disclosure: **H. Lou,** None; **L.-Q. Wu,** None; **H. Wang,** None; **R.-L. Wei,** None; **J.-W. Cheng,** None

References

1. Khong JJ, McNab AA, Ebeling PR, et al. Pathogenesis of thyroid eye disease: review and update on molecular mechanisms. *Br J Ophthalmol*. 2016;100(1):142–150.
2. Bahn RS. Graves' ophthalmopathy. *N Engl J Med*. 2010;363:726–738.
3. Smith TJ, Hegedus L, Douglas RS. Role of insulin-like growth factor-1 (IGF-1) pathway in the pathogenesis of Graves' orbitopathy. *Best Pract Res Clin Endocrinol Metab*. 2012;26:291–302.
4. Kaback LA, Smith TJ. Expression of hyaluronan synthase messenger ribonucleic acids and their induction by interleukin-1beta in human orbital fibroblasts: potential insight into the molecular pathogenesis of thyroid-associated ophthalmopathy. *J Clin Endocrinol Metab*. 1999;84:4079–4084.
5. Zhang L, Bowen T, Grennan-Jones F, et al. Thyrotropin receptor activation increases hyaluronan production in preadipocyte fibroblasts: contributory role in hyaluronan accumulation in thyroid dysfunction. *J Biol Chem*. 2009;284:26447–26455.
6. Ashizawa N, Graf K, Do YS, et al. Osteopontin is produced by rat cardiac fibroblasts and mediates A (II)-induced DNA synthesis and collagen gel contraction. *J Clin Invest*. 1996;98:2218–2227.
7. Uaesoontrachoon K, Yoo HJ, Tudor E, et al. Osteopontin and skeletal muscle myoblasts: Association with muscle regeneration and regulation of myoblast function in vitro. *Int J Biochem Cell Biol*. 2008;40:2303–2314.
8. Ashkar S, Weber GF, Panoutsakopoulou V, et al. Eta-1 (osteopontin): an early component of type-1 (cell-mediated) immunity. *Science*. 2000;287:860–864.
9. Koumas L, Smith TJ, Phipps RP. Fibroblast subsets in the human orbit: Thy-1+ and Thy-1- subpopulations exhibit distinct phenotypes. *Eur J Immunol*. 2002;32:477–485.
10. Wong CK, Lit LC, Tam LS, Li EK, Lam CW. Elevation of plasma osteopontin concentration is correlated with disease activity in patients with systemic lupus erythematosus. *Rheumatology*. 2005;44:602–606.
11. Ambrosi GJ, Catalan V, Ramirez B, et al. Plasma osteopontin levels and expression in adipose tissue are increased in obesity. *J Clin Endocrinol Metab*. 2007;92:3719–3727.
12. Xu L, Ma X, Wang Y, et al. The expression and pathophysiological role of pathophysiological osteopontin in Grave's disease. *J Clin Endocrinol Metab*. 2011;96:1866–1870.
13. Chabas D, Baranzini SE, Mitchell D, et al. The influence of the proinflammatory cytokine, osteopontin, on autoimmune demyelinating disease. *Science*. 2001;294:1731–1735.
14. Vogt MH, Lopatinskaya L, Smits M, et al. Elevated osteopontin levels in active relapsing-remitting multiple sclerosis. *Ann Neurol*. 2003;53:819–822.
15. Urtasun R, Lopategi A, George J, et al. Osteopontin, an oxidant stress sensitive cytokine, up-regulates collagen-I via integrin alpha(V)beta(3) engagement and PI3K/pAkt/NFkappaB signaling. *Hepatology*. 2012;55(2):594–608.
16. Reza S, Shaukat A, Arain TM, et al. Expression of osteopontin in patients with thyroid dysfunction. *PLoS One*. 2013;8(2):e56533.
17. Danese S, Fiocchi C. Platelet activation and the CD40/CD40 ligand pathway: mechanisms and implications for human disease. *Crit Rev Immunol*. 2005;25:103–121.
18. Hwang CJ, Afifiyan N, Sand D, et al. Orbital fibroblasts from patients with thyroid-associated ophthalmopathy overexpress CD40:CD154 hyperinduces IL-6, IL-8, and MCP-1. *Invest Ophthalmol Vis Sci*. 2009;50:2262–2268.
19. Qi Y, Li X, Ma X, et al. The role of osteopontin in the induction of the CD40 ligand in Graves' disease. *Clin Endocrinol (Oxf)*. 2014;80(1):128–134.
20. Dai J, Peng L, Fan K, et al. Osteopontin induces angiogenesis through activation of PI3K/AKT and ERK1/2 in endothelial cells. *Oncogene*. 2009; 28(38):3412–3422.
21. Wang Y, Yan W, Lu X, et al. Overexpression of osteopontin induces angiogenesis of endothelial progenitor cells via the avβ3/PI3K/AKT/eNOS/NO signaling pathway in glioma cells. *Eur J Cell Biol*. 2011;90(8):642–648.
22. Bartley GB, Gorman CA. Diagnostic criteria for Graves' ophthalmopathy. *Am J Ophthalmol*. 1995;119(6):792–795.
23. Bartalena L, Baldeschi L, Dickinson A, et al. Consensus statement of the European Group on Graves' orbitopathy (EUGOGO) on management of GO. *Eur J Endocrinol*. 2008;158(3):273–285.
24. De Carli M, D'Elios MM, Mariotti S, et al. Cytolytic T cells with Th1-like cytokine profile predominate in retroorbital lymphocytic infiltrates of Graves' ophthalmopathy. *J Clin Endocrinol*. 1993;77(5):1120–1124.
25. Hiromatsu Y, Yang D, Bednarczuk T, Miyake I, Nonaka K, Inoue Y. Cytokine profiles in eye muscle tissue and orbital fat tissue from patients with thyroid-associated ophthalmopathy. *J Clin Endocrinol*. 2000;85(3):1194–1199.

26. Wakelkamp IM, Bakker O, Baldeschi L, Wiersinga WM, Prummel MF. TSH-R expression and cytokine profile in orbital tissue of active vs. inactive Graves' ophthalmopathy patients. *Clin Endocrinol (Oxf)*. 2003;58:280–287.
27. Weigel PH, Hascall VC, Tammi M. Hyaluronan synthases. *J Biol Chem*. 1997;272(22):13997–40000.
28. Lund SA, Giachelli CM, Scatena M. The role of osteopontin in inflammatory processes. *Journal of Cell Communication and Signaling*. 2009;3:311–322.
29. Murugaiyan G, Mittal A, Weiner HL. Identification of an IL-27/osteopontin axis in dendritic cells and its modulation by IFN-gamma limits IL-17-mediated autoimmune inflammation. *Proc Natl Acad Sci USA*. 2010;107:11495–11500.
30. Denhardt DT, Noda M, O'Regan AW, Pavlin D, Berman JS. Osteopontin as a means to cope with environmental insults: regulation of inflammation, tissue remodeling, and cell survival. *J Clin Invest*. 2001;107:1055–1061.
31. Weber GF, Ashkar S, Glimcher MJ, Cantor H. Receptor-ligand interaction between CD44 and osteopontin (Eta-1). *Science* 1996;271:509–512.
32. Wai PY, Kuo PC. The role of OPN in tumor metastasis. *J Surg Res*. 2004;121:228–241.
33. Van Steensel L, Dik WA. The orbital fibroblast: a key player and target for therapy in Graves' ophthalmopathy. *Orbit*. 2010;29(4):202–206.
34. Cao HJ, Wang HS, Zhang Y, Lin HY, Phipps RP, Smith TJ. Activation of human orbital fibroblasts through CD40 engagement results in a dramatic induction of hyaluronan synthesis and prostaglandin endoperoxide H synthase-2 expression: insights into potential pathogenic mechanisms of thyroid-associated ophthalmopathy. *J Biol Chem*. 1998;273(45):29615–29625.
35. Smith TJ. Novel aspects of orbital fibroblast pathology. *J Endocrinol Investig*. 2004;27:246–253.
36. Zhao LQ, Wei RL, Cheng JW, Cai JP, Li Y. The expression of intercellular adhesion molecule-1 induced by CD40-CD40L ligand signaling in orbital fibroblasts in patients with Graves' ophthalmopathy. *Invest Ophthalmol Vis Sci*. 2010;51:4652–4660.
37. Wang H, Zhu L-S, Cheng J-W, et al. CD40 ligand induces expression of vascular cell adhesion molecule 1 and E-selectin in orbital fibroblasts from patients with Graves' orbitopathy. *Graefes Arch Clin Exp Ophthalmol*. 2015;253:573–582.
38. Zhang L, Grennan-Jones F, Lane C, Rees DA, Dayan CM, Ludgate M. Adipose tissue depot-specific differences in the regulation of hyaluronan production of relevance to Graves' orbitopathy. *J Clin Endocrinol Metab*. 2012;97(2):653–662.
39. Martins JR, Furlanetto RP, Oliveira LM, et al. Comparison of practical methods for urinary hyaluronan with clinical activity scores in patients with Graves' ophthalmopathy. *Clin Endocrinol (Oxf)*. 2004;60(6):726–733.
40. Li X, Qi Y, Ma X, et al. Chemokine (C-C motif) ligand 20, a potential biomarker for Graves' disease, is regulated by osteopontin. *PLoS One*. 2013;8(5):e64277.
41. Antonelli A, Ferrari SM, Fallahi P, et al. Cytokines (interferon-γ and tumor necrosis factor-α)-induced nuclear factor-κB activation and chemokine (C-X-C motif) ligand 10 release in Graves disease and ophthalmopathy are modulated by pioglitazone. *Metabolism*. 2011;60(2):277–283.
42. Gillespie EF, Raychaudhuri N, Papageorgious KI, et al. Interleukin-6 production in CD40-engaged fibrocytes in thyroid-associated ophthalmopathy: involvement of Akt and NF-KB. *Invest Ophthalmol Vis Sci*. 2012;53(12):7746–7753.
43. Luo L-H, Li D-M, Wang Y-L, et al. Tim3/galectin-9 alleviates the inflammation of TAO patients via suppressing Akt/NF-kB signaling pathway. *Biochem Biophys Res Commun*. 2017;491(4):966–972.
44. Diana T, Olivo PD, Kahaly GJ. Thyrotropin Receptor Blocking Antibodies. *Horm Metab Res*. 2018;50(12):853–862.
45. Heufelder AE. Pathogenesis of Graves' ophthalmopathy. *Z Arztl Fortbild Qualitatssich*. 1999;93:35–39.
46. Ye S, Liu J, Wang Y, Bin Y, Wang J. Increased serum VEGF and b-FGF in Graves' ophthalmopathy. *Graefes Arch Clin Exp Ophthalmol*. 2014;252:1639–1644.
47. Matos K, Manso PG, Marback E, Furlanetto T, Alberti GN, Nosé V. Protein Expression of VEGF, IGF-1 and FGF in Retroocular Connective Tissues and Clinical Correlation in Graves' Ophthalmopathy. *Arq Bras Oftalmol*. 2008;71(4):486–492.
48. Dai J, Peng L, Fan K, et al. Osteopontin induces angiogenesis through activation of PI3K/AKT and ERK1/2 in endothelial cells. *Oncogene*. 2009;28:3412–3422.

Investigative Ophthalmology & Visual Science